Solar Energy Materials & Solar Cells 248 (2022) 112024

Contents lists available at ScienceDirect

Solar Energy Materials and Solar Cells

journal homepage: www.elsevier.com/locate/solmat

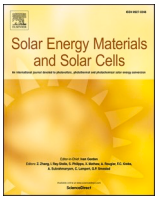

Copper in compensated p- and n-type Czochralski silicon: Diffusivity, influence on the majority charge carrier density and mobility

G. Gaspar [a,b,*], C. Modanese [a,1], S. Bernardis [c], N. Enjalbert [c], L. Arnberg [a], S. Dubois [c], M. Di Sabatino [a]

[a] Department of Materials Science and Engineering, Norwegian University of Science and Technology (NTNU), 7491, Trondheim, Norway
[b] Instituto Dom Luiz, Faculdade de Ciências, Universidade de Lisboa, 1749-016, Lisboa, Portugal
[c] Université Grenoble Alpes, CEA, LITEN, INES, 73375, Le Bourget du Lac, France

ARTICLE INFO

Keywords:
Silicon
Czochralski
Compensation
Copper
Diffusivity
Majority carrier mobility

ABSTRACT

Copper contamination risks are present throughout the whole crystalline silicon solar cell process flow, namely during ingot growth processes using recycled feedstock, wafer sawing and metallisation. Copper is a fast-diffusing impurity which can modify the carrier transport and recombination properties. The aim of this study is to present new insights into the properties of copper-contaminated highly doped and compensated silicon, with a focus on the copper diffusivity and the influence of this impurity on the majority carrier mobility and density. For this, compensated Czochralski silicon ingots were grown from electronic grade feedstock doped with boron and phosphorus, and the wafers intentionally contaminated with copper. Its concentrations were measured by Glow Discharge Mass Spectrometry, while the electrical properties were extracted from Hall Effect measurements. The dopant concentrations were used to compute the effective diffusivity of interstitial copper and important changes in the copper diffusivity are expected in the vicinity of the p-type/n-type transition. For the n-type compensated wafers, a strong migration of copper atoms towards the surface and a reduced copper bulk content were highlighted. Furthermore, the presence of precipitates was experimentally revealed. Both the equilibrium electron density and electron mobility were not influenced by the contamination. In p-type compensated material, copper atoms did not accumulate at the surface, probably due to both the limited copper precipitation in p-type silicon and the lower copper diffusivity. In addition, the equilibrium hole density was not influenced. However, the hole carrier mobility was affected, likely associated to the higher bulk copper content.

1. Introduction

Copper (Cu) is an impurity often present during crystalline silicon (Si) solar cells manufacturing [1], because of its incorporation during the ingot growth [2], surface contamination during ingot sawing and wafer texturing [3–5] and contamination risks due to the use of Cu-based electric contacts [6]. For instance, Cu concentrations ([Cu]) as high as 1×10^{13} cm^{-3} have been found in multicrystalline Si wafers obtained by directional solidification [7]. In that case, Cu essentially came from the silica crucible and its silicon nitride coating [2,8,9]. Cu is a fast-diffusing impurity, i.e. Cu can easily diffuse through the thickness of a solar cell or a Si block within a few hours to several days at room temperature [8,10], which makes the understanding of its behaviours in solid Si of utmost importance to reduce the Cu effect on both bulk and emitter electrical properties degradations. For instance, Cu can be redistributed during device fabrication through external gettering towards the solar cell phosphorus-diffused emitter. However, this phenomenon seems to be more efficient if the wafer is cooled down over a specific temperature range (600-800 °C) [11]. Coletti et al. [12] have intentionally Cu-contaminated Si ingots and demonstrated that concentrations above 1.7×10^{17} cm^{-3} at the wafer level lead to an increase in the recombination activity in both the solar cell emitter and bulk. Also, Modanese et al. [13] have intentionally contaminated p-type wafers with Cu for further PERC solar cells manufacturing with the aim of assessing the impact of Cu on the light-induced degradation (LID) phenomena. Besides showing that the Cu concentration has a direct influence on Cu-LID, they reported that PERC cells are more sensitive to such a contaminant when compared to Al-BSF solar cells. Nevertheless,

* Corresponding author. Instituto Dom Luiz, Faculdade de Ciências, Universidade de Lisboa, 1749-016, Lisboa, Portugal.
E-mail address: gmgaspar@fc.ul.pt (G. Gaspar).
[1] Currently at ElFys Inc., Tekniikantie 12, 02150 Espoo, Finland.

https://doi.org/10.1016/j.solmat.2022.112024
Received 22 May 2022; Received in revised form 5 September 2022; Accepted 17 September 2022
Available online 4 October 2022

Cu-based contacts are progressively seen as a viable alternative to silver-based pastes in Si heterojunction solar cells due to their high conductivity and required lower finger width [14]. Recently, electroplating of Cu-based contacts has been proved to be a suitable solution to metallize bifacial TOPCon solar cells leading to significant cost reductions [15]. The potential diffusion of Cu from the plated metallization into Si bulk may also require the introduction of a diffusion barrier [16] as well as deep knowledge on how this impurity deteriorates the electrical properties of the devices.

Several research groups have studied the behaviour of Cu in uncompensated Si by intentional contamination, both in p-type [17–25] and n-type [22,26] Si. Istratov et al. [20] calculated the diffusivity of Cu in intrinsic Si and predicted a diffusion length of ~3.5 mm for a 10 min long anneal at 900 °C. Moreover, the Cu solid solubility in Si is highly temperature dependent [27]: at 900 °C it is approximately 2×10^{17} cm^{-3} while only in the order of 10^{14} cm^{-3} at 500 °C. Also, Cu is known to diffuse towards areas of higher chemical potential, such as extended defects and surfaces [28]. Regarding its influence on the charge carrier lifetime (τ), interstitial Cu (Cu_i) is a shallow donor with relatively modest electrical activity [29]. On the other hand, Cu precipitates are known to severely affect τ by forming bands of energy states within the Si bandgap, thereby providing very effective pathways for recombination [30]. Cu precipitates are mostly found in Si as Cu_3Si. They may form and grow when the charge state of Cu_i changes from positive to negative/neutral since Cu precipitates are usually positively charged [16]. The precipitation of Cu is favoured in n-type Si since in this material Cu_i is usually neutral or negatively charged.

In parallel, the production of low-cost Si purified via metallurgical routes and the use of feedstock from recycling processes are identified as both carbon footprint and cost reduction opportunities for the terawatt-scale photovoltaic industry [31]. However, these approaches can lead to extra challenges in controlling metal impurities like Cu. With such feedstock, Si wafers can also feature high and similar concentrations of both Boron (B) and Phosphorus (P), which can lead to modified electrical properties. For instance, dopant compensation can lead to a considerable reduction in carrier mobility. The presence of different amounts of B and P can also influence the intrinsic behaviour of Cu in Si, and thus impacts the overall ingot quality.

Even if Cu is one of the main metal impurities in Si, its influence on the properties of highly doped and compensated materials has been rarely studied. Therefore, the main goal of this study is to bring new insights into the effect of Cu on the compositional and electrical properties of highly doped and compensated p-type and n-type Si. More precisely, this study focuses on the Cu diffusivity in such materials and on the influence of the Cu contamination on the majority carrier density and mobility.

2. Materials and methods

The wafers presented in this work were taken from a compensated Czochralski (Cz) Si ingot, grown from an electronic-grade feedstock, deliberately contaminated with B and P. The addition of these elements was defined in order to observe a change in the type of conductivity, which was located at about 77% of the ingot's height. The B and P concentrations ([B] and [P] respectively) along the height of the ingot were accurately determined by the combination of various chemical – Glow Discharge Mass Spectrometry (GDMS) and Inductively Coupled Plasma Mass Spectrometry (ICPMS) – and electrical (temperature-dependent Hall Effect) analyses. The concentration distribution of both dopant species versus ingot height and the corresponding net doping are shown in Fig. 1. p_0 values (net doping or majority carrier concentrations) were computed from [B] and [P], by taking into account the incomplete ionization of the B and P atoms in p-type and n-type Si, respectively, and by considering the variation of the dopants' energy levels with their concentration (see section 3.1. for more details). The selected 4-inch wafers, with thicknesses between 360 μm and 445 μm, were taken from both the p-type and the n-type regions. For this Cz ingot, the total Oxygen (O) and Carbon (C) concentrations ([O] and [C], respectively) were determined by Secondary Ion Mass Spectroscopy (SIMS). In addition, a reference wafer was selected from a B-doped Cz ingot grown from an electronic-grade feedstock. The materials investigated in this work, with their doping levels, compensation ratios (R_c) and light impurity concentrations are reported in Table 1.

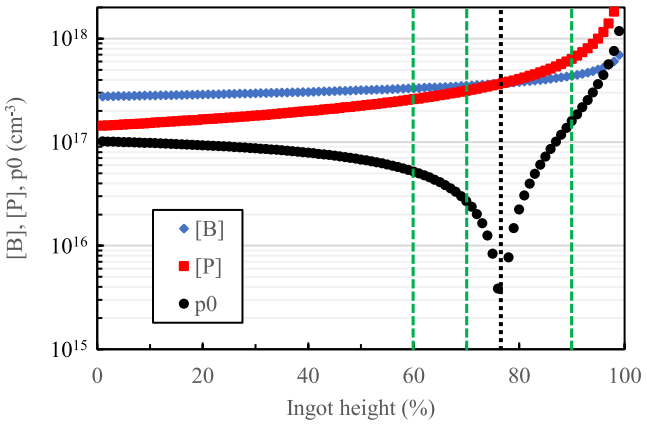

Fig. 1. B and P concentrations as well as the equilibrium majority carrier concentration (shown as p_0, independently of the conductivity type) as a function of the ingot's height. The black dashed line corresponds to the transition between p- and n-type Si while the green ones represent the different locations where the samples were extracted for this study. (For interpretation of the references to colour in this figure legend, the reader is referred to the Web version of this article.)

Prior to Cu contamination, the wafers were double-side mirror polished down to 1 μm, which corresponds to the final surface roughness.

Table 1
Doping levels, compensation ratios and light-element concentrations of the investigated materials.

Sample	Solid fraction	Cu contamination	[B] (cm^{-3})	[P] (cm^{-3})	$R_C = \lvert [B]+[P] \rvert / \lvert [B]-[P] \rvert$	Light elements (cm^{-3})
307c	0.6	Yes	3.3×10^{17}	2.6×10^{17}	8.4	[O] ≈ 6.9×10^{17} [C] ≈ 8.6×10^{16}
311b	0.6	No	3.3×10^{17}	2.6×10^{17}	8.4	[O] ≈ 6.9×10^{17} [C] ≈ 8.6×10^{16}
372c	0.7	Yes	3.6×10^{17}	3.4×10^{17}	35	[O] ≈ 7.7×10^{17} [C] ≈ 1.2×10^{17}
457c	0.9	Yes	4.4×10^{17}	6.4×10^{17}	5.4	[O] ≈ 7.5×10^{17} [C] ≈ 9.4×10^{16}
458b	0.9	No	4.4×10^{17}	6.4×10^{17}	5.4	[O] ≈ 7.5×10^{17} [C] ≈ 9.4×10^{16}
162c	0.3	Yes	1.6×10^{16}	–	1.0	[O] ≈ 7.0×10^{17} [C] ≈ 1.1×10^{16}
162b	0.3	No	1.6×10^{16}	–	1.0	[O] ≈ 7.0×10^{17} [C] ≈ 1.1×10^{16}

Samples were Cu-contaminated with 3 mol/L Cu(II) nitrate trihydrate, $Cu(NO_3)_2{\cdot}3H_20$, dissolved in DI water. The solution was spread on the backside of the wafers and then the wafers baked on a hot plate at 60 °C in air until the solution dried. Afterwards, the wafers were heated in a tube furnace at 900 °C in Ar atmosphere for 30 min in order for the Cu atoms to diffuse into the wafer. The samples were then quickly removed from the furnace and quenched in air with an estimated cooling rate of 3.5–7.0 °C/s. Although relatively high cooling rates were employed, the formation of Cu-silicide precipitates during the cooling stage cannot be totally ruled out. Immediately after the cooling, the excess Cu residuals at the surface were mechanically removed. The polishing was shallow in order to avoid removing Cu that had diffused toward the surface. A similar procedure was previously used by Hu et al. [32], where the Cu concentration at the sample surface is expected to reach values higher than 2.2×10^{17} cm^{-3}.

The contaminated wafers were then laser cut into smaller square pieces (20×20 mm^2) for electrical and chemical characterizations. The different square pieces were selected from the central region of the wafer to ensure similar chemical compositions and defect densities. Table 2 summarizes the sample preparation procedure. The control samples, i.e. the non-Cu-contaminated ones, did not undergo steps 2 and 3.

For the contaminated wafers, [Cu] was analysed by GDMS 4 days after the end of the annealing, over a total depth of ~15 μm and with a depth resolution of ~0.5 μm. Measurements and the resulting semi-quantitative results (as Ion Beam Ratio) are obtained according to Ref. [33] and Cu concentrations profiles are further computed to cm^{-3}. Notice that the GDMS analyses give the total concentration of Cu, i.e. both dissolved and precipitated Cu. Thus, the depth profiles presented in this work refer to the total Cu concentrations.

Hall Effect measurements were carried out at room temperature on an Ecopia HMS 3000, with a Van der Pauw contact configuration, ten days after the samples have been Cu contaminated. For each measurement, ohmic contacts were formed by mechanically embedding liquid Indium–Gallium (InGa) at the corners of the sample. The resistivity (ρ), the Hall majority carrier density (p_{Hall} for p-type Si and n_{Hall} for n-type Si) were measured and then the Hall majority carrier mobility (μ_{Hall}) extracted. The p_0 and n_0 values were further computed with a Hall factor $r_H = 0.77$ as used in previous works [34,35]. Since the goal of this study was not to extract the absolute p_0 and n_0 values, but rather to assess the influence of the Cu contamination on this parameter, we neglected the effects of both the dopant concentrations and the conductivity type on r_H.

Since different areas of the initial 4-inch wafers were selected for measurements, the spatial distribution of the majority carrier density was evaluated by carrier density imaging (CDI) at a temperature of 60 °C. The majority carrier density values measured on the areas corresponding to the pieces used for this study reveal that the average values for the different areas deviate by up to 2.7%, and that the standard deviation within a single piece is maximum of 6.3%. Consequently, the materials used for e.g. Hall Effect measurements feature acceptable properties in terms of homogeneity (at least, in respect to carrier density).

Table 2
Cu contamination procedure.

Step	Description
1	Double-side mechanical polishing
2	Cu contamination
3	Drying at 60 °C, 1.5–2 h, air atmosphere
4	Annealing at 900 °C, 30 min, Ar atmosphere Cooling to RT at 3.5–7 °C/s
5	Removal of excess Cu from the contaminated surface
6	Laser cutting (20×20 mm^2)
7	Storage in dark

3. Results and discussion

3.1. Cu diffusivity in compensated silicon

In order to analyze the experimental results, particularly the [Cu] profiles revealed by GDMS analyses, the Cu diffusivity (D_{Cui}) in highly doped and compensated Si is an important matter that has to be discussed. Cu diffuses interstitially in Si [36]. Cu_i introduces a donor energy level (E_{Cui}) in the Si band gap located at 0.15 eV below the conduction band, E_C (i.e. E_c-0.15 eV) [37]. Therefore, if the Fermi level (E_F) is below this energy level, Cu_i atoms are essentially positively charged (Cu_i^+). On the other hand, if E_F is above this energy level, most Cu_i atoms are neutral (Cu_i^0). In Si containing B atoms, Cu_i^+ interacts with ionized B (B^-). This electrostatic attraction reduces the Cu_i^+ diffusivity. On the other hand, in intrinsic Si and non-compensated n-type Si, Cu_i features a high diffusivity (D_{int}) independently of its charge state (i.e. no interactions with acceptor dopants), given by the following expression (in $cm^2{\cdot}s^{-1}$) [38]:

$$D_{int} = (3.0 \pm 0.3) \times 10^{-4} \times \exp(-0.18 \pm 0.01 eV / k_B T) \quad (1)$$

where k_B is the Boltzmann constant and T the temperature in K. If Cu_i is positively charged and the material contains ionized B atoms, the Cu diffusivity – usually called the effective diffusivity (D_{eff}) – can be significantly lower and is given by the following expression (in $cm^2{\cdot}s^{-1}$) [38]:

$$D_{eff} = \frac{3 \times 10^{-4} \times \exp(-2090/T)}{1 + 2.584 \times 10^{-20} \times \exp(4990/T)([B]/T)} \quad (2)$$

where T is the temperature in K and [B] is the B concentration expressed in cm^{-3}. This expression is valid for low T (below 107 °C) and usually for [B] lower than 1×10^{17} cm^{-3}. For [B] higher than 1×10^{17} cm^{-3}, a non-negligible fraction of B atoms can remain unionized in p-type Si, due to the proximity of E_F and the B energy level (E_B). This means that in highly doped p-type Si, [B^-] (the concentration of ionized B atoms) can differ from [B]. Therefore, for [B] higher than 1×10^{17} cm^{-3}, [B] should be replaced by [B^-] in Equation (2). Notice that in a B-compensated n-type Si, it is assumed that [B^-] = [B] as the B energy level is far below E_F. To assess the amount of incomplete ionization we used the following expression based on the neutrality equation combined with Fermi-Dirac statistics:

$$p_0 = [B^-] - [P^+] = \frac{[B]}{1 + 4 \times \exp\left(\frac{E_B - E_F}{kT}\right)} - [P] \quad (3)$$

In uncompensated Si, E_B is known to decrease from its low-doping value (E_B = 44.4 meV, as measured from the top of the valence band) when [B] exceeds a limit value of approximately 2×10^{17} cm^{-3}, as presented by Altermatt et al. [39]. In the studied compensated samples, [B] exceeds 3×10^{17} cm^{-3} (see Table 1) and is therefore above this limit value. Consequently, we adapted Equation (3) to take into account the variation of E_B with [B], according to the values from Ref. [39]. We neglected the effects of the dopant compensation on the variation of E_B with [B]. For the studied p-type Si, the computed [B^-], p_0 and E_F values are presented in Table 3. In p-type Si, it is assumed that all the Cu_i atoms are positively charged (E_{Cui} is far above E_F). The D_{Cui} values are calculated from the computed [B^-] ones using Equation (2) and are presented in Table 3. For compensated n-type Si, the charge state of Cu_i atoms has to be assessed to determine the Cu_i diffusivity. For the studied n-type sample, the majority carrier concentration (n_0) and E_F are computed using the following expression based on the neutrality equation combined with Fermi-Dirac statistics:

$$n_0 = [P^+] - [B^-] = \frac{[P]}{1 + 2 \times \exp\left(\frac{E_F - E_P}{kT}\right)} - [B] \quad (4)$$

For this computation, the variation of the energy level introduced by

Table 3
Calculated Fermi level energy (E_F) and effective diffusivity of Cu_i (D_{Cui}) for the samples investigated in this study.

Sample	Type	[B] (cm^{-3})	[P] (cm^{-3})	[B^-] (cm^{-3})	p_0, n_0 (cm^{-3})	E_F (eV)	D_{Cui} ($cm^2.s^{-1}$)
307c	p	3.3×10^{17}	2.6×10^{17}	3.2×10^{17}	5.6×10^{16}	E_v+0.15	6.1×10^{-10}
372c	p	3.6×10^{17}	3.4×10^{17}	3.6×10^{17}	1.5×10^{16}	E_v+0.18	5.5×10^{-10}
457c	n	4.4×10^{17}	6.4×10^{17}	4.4×10^{17}	1.7×10^{17}	E_c-0.13	2.8×10^{-7}
162c	p	1.6×10^{16}	–	1.6×10^{16}	1.6×10^{16}	E_v+0.18	1.2×10^{-8}

the P atoms (E_P) with [P] is taken into account using the values from Ref. [39]. The computed E_F and n_0 values are presented in Table 3. For the studied n-type sample, E_F is located at 132 meV below E_C, therefore, E_F is in the vicinity of E_{Cui} (located at 150 meV below E_C). Thus, in order to precisely assess the amount of neutral and positively charged Cu_i atoms, Fermi-Dirac statistics are used:

$$\frac{[Cu_i^+]}{[Cu_i^0]} = 0.5 \times \exp\left(\frac{E_{Cui} - E_F}{kT}\right) \quad (5)$$

The ratio $[Cu_i^+]/[Cu_i^0]$ is equal to 0.25. This means that the Cu_i atoms would be essentially neutral in the studied n-type compensated Si sample. Therefore, since the electrostatic interactions between the Cu_i and B atoms should be limited, D_{Cui} was computed using Equation (1) for this sample, and the results are presented in Table 3. Interestingly, the D_{Cui} values are strongly different for p- and n-type compensated samples, with values significantly lower for the p-type wafers. This feature is particularly remarkable for the p- and n-type samples coming from the vicinity of the conductivity type transition, although these samples have similar compositional properties.

3.2. Cu concentration profiles

The concentration profile of Cu in the contaminated wafers was measured by GDMS over a depth of ~15 μm (see Fig. 2). The measured values are, in general, within the same order of magnitude of bulk Cu concentrations found in other studies relying on similar thermal processes [28,40].

The Cu depth profile of the p-type compensated sample (372c) reveals three different regions: 1) absence of Cu surface accumulation (first 2 μm); 2) a moderately flat distribution until ca. 7 μm; and 3) a subsequent decrease until 15 μm (maximum depth). On the other hand, the n-type compensated sample (457c) shows higher concentrations towards the surface and a steeper decrease with increasing depth, i.e. decreasing to the power of 1.5. The p-type non-compensated sample (162c) shows a depleted region below the surface, and an almost linear decrease with increasing depth after the end of the depleted region. In this work, the Cu concentration was not measured on the corresponding uncontaminated wafers. However, the ingots are solidified from electronic grade Si feedstock; hence, low Cu concentrations are expected in the as-grown wafers.

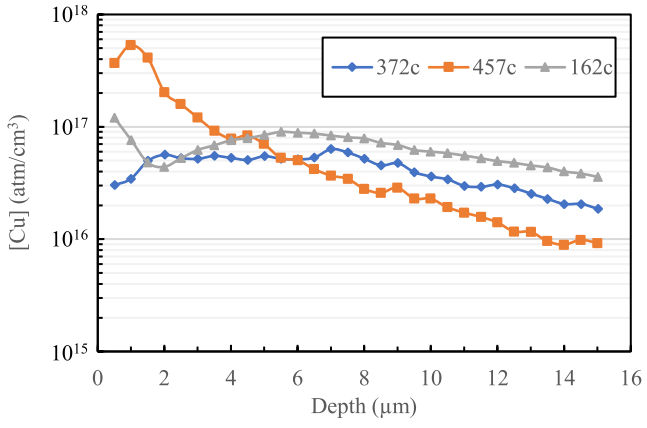

Fig. 2. Cu concentration versus sample depth (from the surface), as measured by GDMS, four days after contamination. 372c, 457c and 162c stand for compensated p-type, compensated n-type and non-compensated p-type Si, respectively.

The integral of the concentration over the 15 μm depth is in the same order of magnitude for all samples, and corresponds to 6.2×10^{13}, 1.3×10^{14} and 9.6×10^{13} cm^{-2} for samples 372c, 457c and 162c, respectively. In addition, the slope of the curves for depths below 4 μm seem to change from sample to sample. For the n-type compensated Si sample, and besides the higher Cu accumulation at its near surface, the slope of the corresponding Cu depth profile is the highest among the different samples. Although the sample processing steps have been kept similar for all samples, the GDMS results show that the [Cu] spatial distribution can be significantly different from one sample to the other, depending on their dopants contents.

The spatial distribution of Cu atoms after the in-diffusion annealing, the cooling step and subsequent storage, is governed by several mechanisms (e.g. out-diffusion, bulk and surface precipitation), which depend on various factors (e.g. Cu diffusivity, surface states, Fermi level position and cooling rate). A comprehensive explanation of the different Cu spatial distributions would therefore require further analyses combining computational approaches and complementary characterizations (particularly to distinguish precipitated Cu from Cu_i). Below, we propose a preliminary explanation relying on both precipitates' observations in the n-type compensated sample and the computed Cu diffusivity values.

Focusing on the Cu-contaminated n-type compensated samples, the GDMS data highlighted a Cu accumulation at the wafer surface. The formation of Cu precipitates was observed in this n-type compensated sample after selective chemical etching. Fig. 3 shows infrared microscopy images of uncontaminated (left) and Cu contaminated (right) n-type compensated etched samples. It is possible to observe an increase in the etch pit density from approximately 2.5×10^4 to 1.6×10^5 cm^{-2} after Cu contamination. Despite the potential formation of some Cu precipitates during samples' cooling, the increase of the etch pit density in such n-type wafers is believed to be mainly related to the strong Cu out-diffusion and further Cu precipitates development close to the surface due to the lack of electrostatic repulsion between the two Cu states (i.e. Cu_i and Cu precipitates). Cu precipitation close to the surface would act as the driving force for the migration of Cu_i atoms from the Si bulk to the surface, explaining the decrease of the Cu concentration with depth. This migration towards the surface strongly depends on the Cu_i diffusivity. We computed the Cu_i diffusion length (defined as $2\sqrt{D_{Cui}t}$, with t corresponding to time [17,41]) for the room temperature storage period, and a value of 6222 μm was obtained for the n-type compensated Si sample (i.e. 457c). Assuming that Cu_i atoms are initially homogeneously distributed in the Si matrix, and that half of the Si wafer average thickness is approximately 201 μm, this confirms that Cu_i atoms could easily migrate to the surface during the storage period. Since the diffusion length is significantly higher than the wafer's thickness, we could expect the Cu atoms to be even more concentrated at the surface (i.e. a flatter concentration profile in the bulk). The calculated Cu diffusion lengths may thus be overestimated. Diffusion models in crystalline Si, and derived diffusion length approximations, follow several assumptions such as an infinite and constant surface source of impurities (e.g. dopant species) and a semi-infinite media [42–44] which are not valid here. Moreover, Cu migration may be retarded by the high bulk [O] and

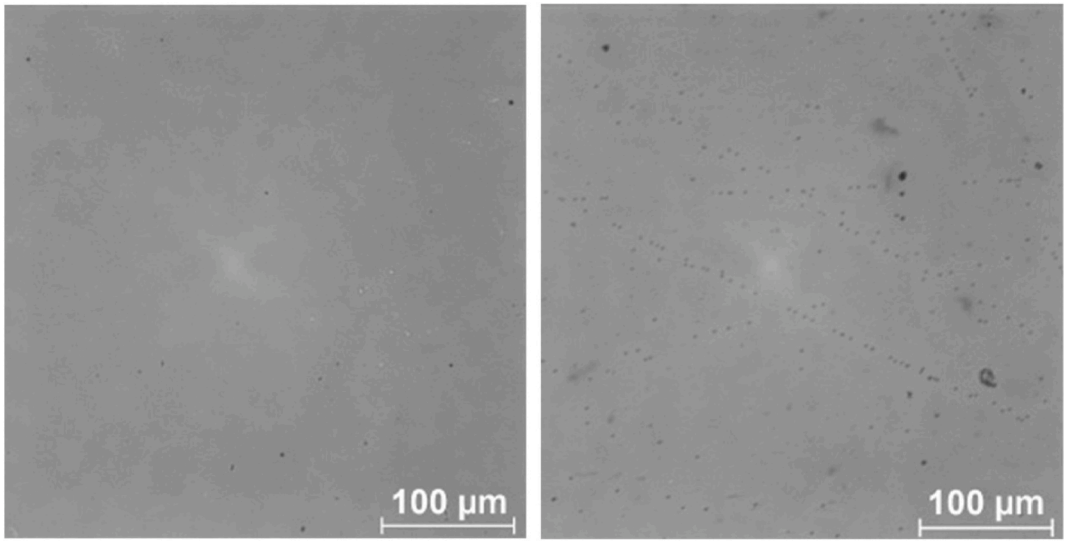

Fig. 3. Infrared microscopy images after etching of uncontaminated (left) and Cu contaminated (right) n-type compensated Si samples.

[C] contents of the samples under investigation. Indeed, Cu diffusivity equations were obtained from Ref. [38], where the models neglected the interaction of Cu_i atoms with both impurities since the study was carried out on FZ samples. In our samples, both [O] and [C] are 1–3 orders of magnitude higher than those typically found in FZ Si. Mesli et al. [45] used a combination of C–V and transient ion drift measurements to determine Cu diffusivity in Si as a function of temperature. To evaluate the impact of interstitial oxygen concentration on the Cu diffusivity, Mesli and co-workers compared Cu-contaminated FZ and Cz samples, which differed in this impurity content by approximately two orders of magnitude (ca. 10^{16} and 10^{18} cm^{-3}, respectively), and found out major reductions in Cu diffusivity due to oxygen at temperatures below 300 K. Thus, even if the storage of our samples was conducted at temperatures close to 300 K, the contribution of oxygen to the reduction of the Cu diffusivity cannot be completely ruled out. On the other hand, studies on the interactions between Cu_i and carbon in crystalline Si, and how this impurity influences the Cu_i diffusivity, are limited. Yet, both local strain and electrostatic interactions between Cu_i and other carbon-related defects in the Si bulk may affect Cu_i diffusivity in carbon-rich Si [46].

Regarding the Cu-contaminated p-type compensated sample, the GMDS data highlighted a rather flat [Cu] profile. First, this may be due to the fact that in p-type Si the Cu precipitation is limited, even at surface defects, due to the electrostatic repulsion between Cu_i atoms and the Cu precipitates. Therefore, the driving force for the Cu migration from the bulk to the surface is probably limited in this material. Following the calculations presented in the previous section, the Cu_i diffusivity for the compensated p-type sample is about 500 times lower than the value found for the highly compensated n-type sample. The computed Cu_i diffusion length for this material corresponds to 276 µm, so that it is in the order of magnitude of the wafer's thickness. Thus, it indicates that an appreciable migration of the Cu_i atoms towards the surface should take place during storage. However, and as discussed above, this diffusion length is probably overestimated and lower diffusion values, preventing the significant surface migration of Cu_i atoms in this material, may be in place. Both mechanisms (i.e. limited precipitation and diffusion) can potentially explain the flatter [Cu] depth profile for this material and the resulting higher Cu content in the Si bulk.

3.3. Hall effect measurements

Room temperature (300 K) resistivity, majority carrier density and Hall mobility are reported in Table 4 for all the samples investigated. The sample with the highest compensation level (sample 372c) was not measurable, A reason for this could be the strong heterogeneities of its electrical properties (i.e. electrostatic potential). Indeed, Shik et al. [47] pointed out that large-scale (i.e. comparable to the sample size) inhomogeneities of the electrostatic potential (usually present in highly compensated materials) could induce biases in the measured Hall voltage. The differences in the output parameters between the Cu contaminated and the blank reference samples for the different materials presented are approaching the accuracy of the measurement technique for most of the studied samples. However, a noticeable influence of Cu on the data extracted from the Hall Effect measurements was observed for the Cu-contaminated p-type compensated sample. The increase in resistivity for the Cu-contaminated p-type compensated sample compared to the associated non-contaminated sample (i.e. 307c compared to 311b) appears to be related mostly to a decrease in carrier mobility rather than to a decrease in majority carrier density. Therefore, the room temperature results show that Cu atoms do not influence the carrier density but can affect the charge carrier mobility.

Table 4
Room temperature resistivity (ρ), Hall majority carrier mobility (μ_{Hall}) and corresponding majority carrier densities (p_0, n_0). Samples 307c, 457c and 162c are contaminated while the others are not.

Sample	ρ (Ω·cm)	μ_{Hall} ($cm^2 \cdot V^{-1} \cdot s^{-1}$)	p_0, n_0 (cm^{-3})
307c	1.1	87	5.9×10^{16}
311b	1.0	101	5.9×10^{16}
457c	0.2	287	8.9×10^{16}
458b	0.2	287	9.3×10^{16}
162c	1.3	287	1.7×10^{16}
162b	1.2	281	1.7×10^{16}

Fig. 4 shows the measured Hall majority carrier mobility as a function of temperature (90–350 K) for p-type compensated (307c), n-type compensated (457c) and p-type non-compensated (162c) contaminated samples as well as for their uncontaminated counterparts (311b, 458b and 162b, respectively). The results show that for temperatures below and above 300 K, there are also no significant differences between the values of the contaminated and uncontaminated samples, except for the p-type compensated sample. In this case, the mobility at 90 K corresponds to 67 and 107 $cm^2 \cdot V^{-1} \cdot s^{-1}$ for contaminated and uncontaminated samples, respectively. These results could be explained by the presence in this material of Cu-related defects (e.g. Cu complexes and precipitates), with a density lower than p_0, but with various ionized energy levels introduced in the Si band gap, enhancing their scattering power (as it is the case for instance for the doubly ionized O-related

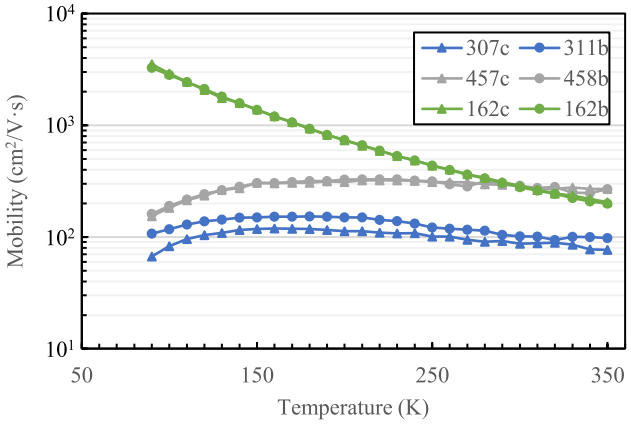

Fig. 4. Temperature dependent Hall majority carrier mobility of Cu contaminated p-type compensated (307c), n-type compensated (457c) and p-type (162c) samples and corresponding uncontaminated ones (311b, 458b and 162b, respectively).

thermal donors in Si, which have a scattering power enhanced by a factor of four compared to a singly-charged donor impurity such as P) [48]. However, this hypothesis should be confirmed by studying samples with higher Cu concentrations.

The effect of the Cu contamination on the studied electrical parameters is thus only observed for the highly doped and compensated p-type sample (sample 307c). In relation to section 3.2, this could be explained by the higher Cu bulk concentration in this sample due to the limited Cu out-diffusion and/or precipitation at the near surface. From the GDMS results, the compensated p-type sample shows lower concentration at the near surface while the compensated n-type sample shows the sharpest Cu depth profile, which confirms the agreement between the results. Furthermore, for the n-type material some Cu-related defects (usually donor) could be non-ionized, with limited scattering capabilities.

4. Conclusions

Highly doped compensated Cz Si samples were intentionally Cu-contaminated in order to investigate the impact of this impurity on Si compositional and electrical properties since it is still one of the most important metal elements present in Si solar cells.

In the studied materials, Cu_i atoms are essentially neutral in n-type compensated Si samples while for the p-type compensated, Cu_i atoms are mostly positively charged. It was possible to conclude from the computed Cu diffusivities that in the vicinity of the p-type to n-type transition in the ingot height, there are important changes in this parameter, reaching values that may be orders of magnitude higher for n-type compensated Si when compared to p-type compensated materials, despite similar compositional properties. GDMS results highlighted a higher [Cu] gradient for n-type compensated Si, with a significant Cu accumulation at the sample surface during storage, as a consequence of both the ability of Cu to form precipitates in such a material and the higher Cu_i diffusivity. On the other hand, no Cu surface accumulation was measured in p-type compensated Si, likely due to the lower Cu diffusivity in this sample and the limited Cu precipitation in p-type Si.

Regarding the Cu effect on the electrical properties, it was possible to conclude that Cu contamination has no impact on the majority carrier density (for the studied [Cu]), and that it only influences the carrier mobility in the highly doped p-type compensated samples. The reduction of the mobility may be due to the higher presence of Cu-related defects in the Si bulk (limited Cu migration towards the surfaces), with strong scattering powers (introduction of various energy levels in the band gap).

CRediT authorship contribution statement

G. Gaspar: Writing – original draft, Methodology, Investigation, Formal analysis, Data curation, Conceptualization. **C. Modanese:** Writing – original draft, Methodology, Investigation, Formal analysis, Data curation, Conceptualization. **S. Bernardis:** Writing – original draft, Methodology, Investigation, Formal analysis, Data curation. **N. Enjalbert:** Methodology, Investigation, Formal analysis, Data curation. **L. Arnberg:** Writing – review & editing, Methodology, Investigation, Formal analysis, Conceptualization. **S. Dubois:** Writing – review & editing, Methodology, Investigation, Funding acquisition, Formal analysis, Data curation, Conceptualization. **M. Di Sabatino:** Writing – review & editing, Methodology, Investigation, Funding acquisition, Formal analysis, Data curation, Conceptualization.

Declaration of competing interest

The authors declare that they have no known competing financial interests or personal relationships that could have appeared to influence the work reported in this paper.

Data availability

Data will be made available on request.

Acknowledgements

The support from the Norwegian FME - SUSOLTECH project (Grant No. 257639) is gratefully acknowledged. This work was also funded by the Portuguese Fundação para a Ciência e a Tecnologia (FCT) I.P./MCTES through national funds (PIDDAC) - UIDB/50019/2020. The authors would like to thank Dr. Jordi Vierman for the valuable discussions and for providing some of the samples with helpful information.

References

[1] G. Stokkan, M. Di Sabatino, R. Søndenå, M. Juel, A. Autruffe, K. Adamczyk, H. V. Skarstad, K.E. Ekstrøm, M.S. Wiig, C.C. You, H. Haug, M. M'Hamdi, Impurity control in high performance multicrystalline silicon, Phys. Status Solidi A 214 (2017), 1700319, https://doi.org/10.1002/pssa.201700319.

[2] T. Buonassisi, A.A. Istratov, M.D. Pickett, J.-P. Rakotoniaina, O. Breitenstein, M. A. Marcus, S.M. Heald, E.R. Weber, Transition metals in photovoltaic-grade ingot-cast multicrystalline silicon: assessing the role of impurities in silicon nitride crucible lining material, J. Cryst. Growth 287 (2006) 402, https://doi.org/10.1016/j.jcrysgro.2005.11.053.

[3] J. Schweckendiek, R. Hoyer, S. Patzig-Klein, F. Delahaye, G. Knoch, H. Nussbaumer, Cleaning in crystalline Si solar cell manufacturing, Solid State Phenom. 195 (2013) 283–288. https://doi.org/10.4028/www.scientific.net/SSP.195.283.

[4] F. Buchholz, E. Wefringhaus, G. Schubert, Metal surface contamination during phosphorus diffusion, Energy Proc. 27 (2012) 287–292, https://doi.org/10.1016/j.egypro.2012.07.065.

[5] K. Joshi, P. Padhamnath, U. Bhandarkar, S.S. Joshi, Surface quality and contamination on Si wafer surfaces sliced using wire-electrical discharge machining, J. Eng. Mater. Technol. 141 (2019), 041013, https://doi.org/10.1115/1.4044374.

[6] A. Kraft, C. Wolf, J. Bartsch, M. Glatthaar, Characterization of copper diffusion in silicon solar cells, Energy Proc. 67 (2015) 93–100, https://doi.org/10.1016/j.egypro.2015.03.292.

[7] A.A. Istratov, E.R. Weber, Physics of copper in silicon, J. Electrochem. Soc. 149 (2002) G21–G30, https://doi.org/10.1149/1.1421348.

[8] E.R. Weber, Impurity Precipitation, Dissolution, Gettering and Passivation in PV Silicon, 2002. NREL - NREL/SR-520-31528.

[9] D. Macdonald, A. Cuevas, A. Kinomura, Y. Nakano, Phosphorus gettering in multicrystalline silicon studied by neutron activation analysis, in: Proceedings of the 29th IEEE PVSC, New Orleans, USA, 2002, p. 285, https://doi.org/10.1109/PVSC.2002.1190514.

[10] G. Gaspar, C. Modanese, H. Schøn, M. Di Sabatino, L. Arnberg, E.J. Øvrelid, Influence of copper diffusion on lifetime degradation in n-type Czochralski silicon for solar cells, Energy Proc. 77 (2015) 586–591, https://doi.org/10.1016/j.egypro.2015.07.084.

[11] A. Inglese, H.S. Laine, V. Vahanissi, H. Savin, Cu gettering by phosphorus-doped emitters in p-type silicon: effect on light-induced degradation, AIP Adv. 8 (2018), 015112, https://doi.org/10.1063/1.5012680.

[12] G. Coletti, P.C.P. Bronsveld, G. Hahn, W. Warta, D. Macdonald, B. Ceccaroli, K. Wambach, N.L. Quang, J.M. Fernandez, Impact of metal contamination in silicon solar cells, Adv. Funct. Mater. 21 (2011) 879–890, https://doi.org/10.1002/adfm.201000849.
[13] C. Modanese, Mt Wagner, F. Wolny, A. Oehlke, H.S. Laine, A. Inglese, H. Vahlman, M. Yli-Koski, H. Savin, Impact of copper on light-induced degradation in Czochralski silicon PERC solar cells, Sol. Energy Mater. Sol. Cells 186 (2018) 373–377, https://doi.org/10.1016/j.solmat.2018.07.006.
[14] J. Yu, J. Li, Y. Zhao, A. Lambertz, T. Chen, W. Duan, W. Liu, X. Yang, Y. Huang, K. Ding, Copper metallization of electrodes for silicon heterojunction solar cells: process, reliability and challenges, Sol. Energy Mater. Sol. Cells 224 (2021), 110993, https://doi.org/10.1016/j.solmat.2021.110993.
[15] B. Grubel, G. Cimiotti, C. Schmiga, S. Schellinger, B. Steinhauser, A.A. Brand, M. Kamp, M. Sieber, D. Brunner, S. Fox, S. Kluska, Progress of plated metallization for industrial bifacial TOPCon silicon solar cells, Prog. Photovolt. 30 (2021) 615–621, https://doi.org/10.1002/pip.3528.
[16] A. Lennon, J. Colwell, K.P. Rodbell, Challenges facing copper-plated metallisation for silicon photovoltaics: insights from integrated circuit technology development, Prog. Photovolt. 27 (2019) 67–97, https://doi.org/10.1002/pip.3062.
[17] T. Buonassisi, M.A. Marcus, A.A. Istratov, M. Heuer, T.F. Ciszek, B. Lai, Z. Cai, E. R. Weber, Analysis of copper-rich precipitates in silicon: chemical state, gettering, and impact on multicrystalline silicon solar cell material, J. Appl. Phys. 97 (2005), 063503, https://doi.org/10.1063/1.1827913.
[18] S. Koh, A. You, T. Tou, Copper diffusivity in boron-doped silicon wafer measured by dynamic secondary ion mass spectrometry, Mater. Sci. Eng. B 178 (2012) 321–325, https://doi.org/10.1016/j.mseb.2012.12.004.
[19] M. Saritas, A. Peaker, Deep states associated with oxidation induced stacking faults in RTA p-type silicon before and after copper diffusion, Solid State Electron. 38 (1995) 1025–1034, https://doi.org/10.1016/0038-1101(95)98671-O.
[20] A.A. Istratov, C. Flink, H. Hieslmair, S.A. McHugo, E.R. Weber, Diffusion, solubility and gettering of copper in silicon, Mater. Sci. Eng. B 72 (2000) 99–104, https://doi.org/10.1016/S0921-5107(99)00514-0.
[21] J. Walter, A. Krause, The influence of oxygen precipitates on the diffusion velocity of copper in the bottom parts of the mc-Si ingots, Energy Proc. 27 (2012) 59–65, https://doi.org/10.1016/j.egypro.2012.07.029.
[22] M. Shabani, T. Yoshimi, H. Abe, Low-temperature out-diffusion of Cu from silicon wafers, J. Electrochem. Soc. 143 (1996) 2025–2029, https://doi.org/10.1149/1.1836943.
[23] A. Belayachi, T. Heiser, J.P. Schunck, S. Bourdais, P. Bloechl, A. Huber, A. Kempf, Optimisation of a combined transient-ion-drift/rapid thermal annealing process for copper detection in silicon, Mater. Sci. Eng. B 102 (2003) 218–221, https://doi.org/10.1016/S0921-5107(02)00735-3.
[24] X.-Q. Li, D.-R. Yang, X.-G. Yu, D.-L. Que, Precipitation and gettering behaviors of copper in multicrystalline silicon used for solar cells, Trans. Nonferrous Metals Soc. China 21 (2011) 691–696, https://doi.org/10.1016/S1003-6326(11)60767-X.
[25] J. Lindroos, M. Yli-Koski, A. Haarahiltunen, H. Savin, Room-temperature method for minimizing light-induced degradation in crystalline silicon, Appl. Phys. Lett. 101 (2012), 232108, https://doi.org/10.1063/1.4769809.
[26] M. Nakamura, S. Murakami, H. Udono, Copper centres in copper-diffused n-type silicon measured by photoluminescence and deep-level transient spectroscopy, Appl. Phys. Lett. 101 (2012), 042113, https://doi.org/10.1063/1.4739470.
[27] A.A. Istratov, E.R. Weber, Electrical properties and recombination activity of copper, nickel and cobalt in silicon, Appl. Phys. A 66 (1998) 123–136, https://doi.org/10.1007/s003390050649.
[28] C. Flink, H. Feick, S.A. McHugo, W. Seifert, H. Hieslmair, T. Heiser, A.A. Istratov, E. R. Weber, Out-diffusion and precipitation of copper in silicon: an electrostatic model, Phys. Rev. Lett. 85 (2000) 4900–4903, https://doi.org/10.1103/PhysRevLett.85.4900.
[29] A.A. Istratov, C. Flink, H. Hieslmair, T. Heiser, E.R. Weber, Influence of interstitial copper on diffusion length and lifetime of minority carriers in p-type silicon, Appl. Phys. Lett. 71 (1997) 2121, https://doi.org/10.1063/1.119355.
[30] A.A. Istratov, H. Hedemann, M. Seibt, O.F. Vyvenko, W. Schröter, T. Heiser, C. Flink, H. Hieslmair, E.R. Weber, Electrical and recombination properties of copper-silicide precipitates in silicon, J. Electrochem. Soc. 145 (1998) 3889, https://doi.org/10.1149/1.1838889.
[31] E. Forniés, C. del Cañizo, L. Méndez, A. Souto, A.P. Vázquez, D. Garrain, UMG silicon for solar PV: from defects detection to PV module degradation, Sol. Energy 220 (2021) 354–362, https://doi.org/10.1016/j.solener.2021.03.076.
[32] Y. Hu, H. Schøn, L. Arnberg, Characterization of defect patterns in Cz silicon slabs by carrier density imaging, J. Cryst. Growth 368 (2013) 6–10, https://doi.org/10.1016/j.jcrysgro.2012.12.029.
[33] M. Di Sabatino, Detection limits for glow discharge mass spectrometry (GDMS) analyses of impurities in solar cell silicon, Measurement 50 (2014) 135–140, https://doi.org/10.1016/j.measurement.2013.12.024.
[34] F. Szmulowicz, Calculation of the mobility and the Hall factor for doped p-type silicon, Phys. Rev. B 34 (1986) 4031–4047, https://doi.org/10.1103/PhysRevB.34.4031.
[35] S. Zhang, C. Modanese, G. Gaspar, R. Sondena, G. Tranell, M. Di Sabatino, Majority carrier mobility of compensated silicon: comparison of room temperature measurements and models, Energy Proc. 92 (2016) 278–283, https://doi.org/10.1016/j.egypro.2016.07.078.
[36] S.K. Estreicher, Rich chemistry of copper in crystalline silicon, Phys. Rev. B 60 (1999) 5375–5382, https://doi.org/10.1103/PhysRevB.60.5375.
[37] A.A. Istratov, H. Heislmair, C. Flink, T. Heiser, E.R. Weber, Interstitial copper-related center in n-type silicon, Appl. Phys. Lett. 71 (1997) 2349–2351, https://doi.org/10.1063/1.120026.
[38] A.A. Istratov, C. Flink, H. Heislmair, E.R. Weber, T. Heiser, Intrinsic diffusion coefficient of interstitial copper in silicon, Phys. Rev. Lett. 81 (1998) 1243–1246, https://doi.org/10.1103/PhysRevLett.81.1243.
[39] P.P. Altermatt, A. Schenk, G. Heiser, A simulation model for the density of states and for incomplete ionization in crystalline silicon. I. Establishing the model in Si: P, J. Appl. Phys. 100 (2006), 113714, https://doi.org/10.1063/1.2386934.
[40] D. Ballutaud, P. de Mierry, M. Aucouturier, E. Darque-Ceretti, Influence of thermal treatments on the distribution of contaminating copper near the surface of silicon: a comparative SIMS and XPS study, Appl. Surf. Sci. 47 (1991) 1–8, https://doi.org/10.1016/0169-4332(91)90096-3.
[41] H. Mehrer, Diffusion in Solids: Fundamentals, Methods, Materials, Diffusion-Controlled Processes, first ed., Springer, Berlin, 2007.
[42] P.M. Fahey, P.B. Griffin, J.D. Plummer, Point defects and dopant diffusion in silicon, Rev. Mod. Phys. 61 (1989) 289–384, https://doi.org/10.1103/RevModPhys.61.289.
[43] J. Bartsch, A. Mondon, K. Bayer, C. Schetter, M. Hörteis, S.W. Glunz, Quick determination of copper-metallization long-term impact on silicon solar cells, J. Electrochem. Soc. 157 (2010) H942–H946, https://doi.org/10.1149/1.3466984.
[44] T. Oku, E. Kawakami, M. Uekubo, K. Takahiro, S. Yamaguchi, M. Murakami, Diffusion barrier property of TaN between Si and Cu, Appl. Surf. Sci. 99 (1996) 265–272, https://doi.org/10.1016/0169-4332(96)00464-3.
[45] A. Mesli, T. Heiser, E. Mulheim, Copper diffusivity in silicon: a re-examination, Mater. Sci. Eng. B 25 (1994) 141–146, https://doi.org/10.1016/0921-5107(94)90215-1.
[46] M. Nakamura, Influence of oxygen and carbon on the formation of the 1.014 eV photoluminescence copper center in silicon crystal, J. Electrochem. Soc. 147 (2000) 796–798, https://doi.org/10.1149/1.1393274.
[47] A.Y. Shik, Electronic Properties of Inhomogeneous Semiconductors, first ed., Gordon and Breach, Amsterdam, 1995.
[48] D. Chattopadhyay, H.J. Queisser, Electron scattering by ionized impurities in semiconductors, Rev. Mod. Phys. 53 (1981) 745, https://doi.org/10.1103/RevModPhys.53.745.